



INTERNATIONAL ATOMIC ENERGY AGENCY
UNITED NATIONS EDUCATIONAL, SCIENTIFIC AND CULTURAL ORGANIZATION



INTERNATIONAL CENTRE FOR THEORETICAL PHYSICS
34100 TRIESTE (ITALY) - P.O. B. 686 - MIRAMARE - STRADA COSTIERA 11 - TELEPHONE: 2240-1
CABLE: CENTRATOM - TELEX 480392-I

H4.SMR.203 - 26

" SPRING COLLEGE ON GEOMAGNETISM AND AERONOMY "

(2 - 27 March 1987)

" Magnetovariational studies: principles"

" Magnetotellurics - I "

" Magnetotellurics - II "

presented by :

B.P. SINGH
Indian Institute of Geomagnetism
Dr.Nanabhoy Moos Road
Colaba
Bombay 400 005
India

These are preliminary lecture notes, intended for distribution to participants only.

Magnetovariational Studies : Principles

2

Summary

The physical and chemical properties of the Earth's interior in the depth range of a few or more kilometers cannot be determined directly and must be inferred, albeit imperfectly, from observations in the accessible regions near or above the surface of the earth. Besides providing information to our basic inquisitiveness to know what lies below the earth's surface, knowledge of its deep interior also tell us the areas prone to earthquakes and the regions which could have potential non - renewable resources. The great relevance of both these informations to the present industrialised society, has resulted in increasing use of magnetovariation (MV) or geomagnetic deep sounding (GDS) - as they are also called alternatively. At this stage itself, it is important to point out the inherent limitation of all these studies, for a physical parameter is being deduced from the effects it produces a few hundred kilometers away. In addition its signal is recorded mixed with host of interfering signals generated by other sources. In spite of this difficulty, techniques have been developed to resolve the physical parameters of the earth's interior.

The terrestrial magnetic field has a large (>99%) component of purely internal origin. Sitting on this are small transient variations originating from currents flowing in ionosphere and beyond. Both, the ambient static field and the transient dynamic field, in their spatial patterns show signatures (in the form of anomalies) of subsurface geological structures. The anomalies in the ambient field have been in use since long in geophysical prospecting. Rather this being the cheapest

method is commonly adopted in reconnaissance work. However, the last three decades have seen considerable use of MV (GDS) also in studies of earth's interior. The two magnetic methods: one using static field and the other dynamic field, have very little in common with each other. The effect of first are related to permeability and of the second to electrical conductivity of the medium. An important point to keep in mind is that with the static field sub-surface layers above Curie isotherm ($\sim 20-40$ km) can only be studied, whereas the dynamic part of the field can probe up to about 1500 km. Depth limit of the first is limited to those regions where permanent magnetisation is possible and of the second to the penetration depth of signals originating from Sun.

The first attempt on calculating the conductivity of crust and mantle of earth using transient geomagnetic variations started with Sir Sydney Chapman (1919). On historical counts it should be mentioned that from the time of last century it was realized that the transient variations recorded on the earth's surface contain signatures of electrical conductivity of the earth's interior, and so possibly could be used to estimate them. Despite so clear an understanding of the process, it took about half a century, even after the pioneering work of Chapman in 1919, for GDS to attain credibility and to enter as an one of contemporary methods of lithological studies.

The greatest limitation which resulted in this slow development of the method has been the very nature of the phenomena itself. The common geophysical concept of separating the observed field into its normal and anomalous part poses problems in GDS. Normally, in geophysical studies, the model of the earth that we envisage is one in which the physical properties depend only on the radial distance from the centre. This variation is assumed to dominate any lateral heterogeneity. The latter

are further taken to be small in magnitude compared with the incipient normal absolute value. Also, the heterogeneities are assumed to be randomly distributed in latitude and longitude, so that their effects on surface observations are equivalent to a random noise in the data. With the above assumption, it is possible to obtain an optimum global model for the measured physical quantity provided data from a global coverage are available. The model can then be used to predict normal surface values. This normal field when subtracted from the observed field gives the anomaly field.

Such a separation of normal and anomalous components is not possible with the GDS data. Under the conditions that exist in upper 500 km of the earth, the electrical conductivity can vary over a range of six orders of magnitude. The anomalous values thereby can be orders of magnitude greater than normal values and not just a small perturbation on them. The lateral heterogeneities are neither random in their distribution nor are small in spatial scale. The oceans are the obvious example of a conductivity anomaly that satisfies neither of the two requirements. Then how do we separate the field into global and local components? Earlier studies circumvented the problem by using those frequency components which penetrate to depths more than 500-600 km. For this class of variations contributions from surface contrasts can be minimised and one can talk of a global average. In this category come solar daily variations, Dst variations, 27-day solar cycles, annual variation, etc. But when the main interest of geosciences centres around earthquake prone areas or location of natural resources, then a method that probes layers deeper than 400-500 km has little use. Then to study the upper layers, came the suggestion to separate the field into internal and

external parts using the technique of potential field theory. Once the internal current distribution has been obtained, the identification of conducting zones is a straight-forward exercise. For a full and exact separation of the potential field into components of external and internal origin, we need measurements of the three components of the geomagnetic field at close enough points and covering the whole surface of the earth. This we do not and can not have. Simplifying approaches have been made and such efforts have given good results. The formal separation (even an approximate one) needs a good network of observatories preferably in a gridded form.

A solution to this complex situation came with the novel concept of Schmucker (1970 described in Bulletin Scripps Institute of Oceanography Vol. 13). The field observed on the earth's surface consists of the external source field plus a medium scale field arising from currents induced in highly conducting mantle, and possibly a small induced current in conducting zones of crust and the oceans. These small scale currents are largely perturbed by anomalous zones of conductivity. Schmucker's separation is not in terms of external and internal components rather he tries only to isolate the perturbed part of the internal field lumping together as normal field the remaining part of the internal currents with the external currents. The field associated with the perturbed part of the internal current is called the anomalous field. He did so on two considerations :

- the normal component has nearly equal contribution from external sources, whereas the anomalous part is purely of internal origin. Thus Z_a (Z - anomalous) and H_a (H - anomalous) are interdependent.

- normal Z-H (i.e. $Z_n \sim H_n$) relations are the same for all directions of polarisation of the source field, whereas, the amplitude of Z_a is critically dependent on the polarisation of the source field in relation to sub-surface lateral conductivity contrasts.

The dependence of Z_a on the polarisation of the source field had been established by two independent works of Parkinson and Wiese. In anomaly studies, the standard procedure now is to calculate induction vectors called by some as Parkinson's vector and by others Wiese vectors. These vectors will be shown later to be very effective in identifying conductivity contrasts.

The conductive zones can also be identified through contour maps of Fourier transform amplitudes. As Fourier transform refers to a precise period and gives an estimate of the sums of energy at that period in the whole event, plots of its amplitudes and phases have proved effective in delineation of conductive zones. The applications of all these techniques will be illustrated by field examples after giving the necessary physical background.

Physical Background

The average conductivity of continental regions at first drops sharply with increasing depth as the influence of conductive sediments, moist surface rocks, and the like decreases. It is probable that the greater part of the crust and then some hundreds of kilometers of mantle have a comparatively low conductivity, of about 10^{-4} sm^{-1} . At a depth of about 500 km the conductivity increases very rapidly, reaching 10^{-1} sm^{-1} at about 700 km, although estimates at these depths become increasingly uncertain. At a depth of 2000 km the conductivity is probably as high as

10^2 sm^{-1} . As a first approximation we can thus regard the uppermost region of the earth as consisting of a very thin and rather irregular surface layer of intermediate to high conductivity underlain by perhaps 500 km of poorly conducting upper mantle, this in turn sitting on the very high conducting lower mantle.

Inhomogeneities may occur in each of these three layers : the surficial conducting layer may be thicker or more highly conducting in some areas than others, or it may virtually vanish in others. The depth to the highly conducting part of mantle may vary, and localized volumes of higher conductivity may be embedded in the poorly conducting upper mantle. We then regard the total conductivity as being made of these smaller-scale three-dimensional inhomogeneities superimposed upon the larger-scale purely radial variation.

Induction in a conductor with purely radial, or one-dimensional, variation in conductivity by an external source field produces a secondary or induced field whose variation with horizontal position is determined by characteristics of the source field. If the characteristic length of the source field is somewhat greater than the depth to the highly conductive part of the mantle, the total field will be the vector sum of the varying source field and the field induced by this in the highly conductive part of the mantle. The sum, termed the normal field, acts upon the smaller scale inhomogeneities in conductivity to produce in them secondary fields (called anomalous fields). It is relevant to point out that internal fields of characteristic lengths greater than the dimension of the array will be included in the normal field.

Typically, the maximum linear dimension of an array of magnetometers does not exceed 2000 km. This distance is substantially greater than

the depth to the highly conductive part of the mantle, though being sufficiently small that the curvature of the surface of the earth across the array is small in comparison with depth. Therefore over the array we can regard the earth as a portion of an infinite half space, the induced part of the normal field being produced in parallel layers of varying conductivity within the half space.

Let the half space occupy the region $Z > 0$, and assume that the primary field has its origin in the region $Z < h < 0$, using Cartesian coordinates (X, Y, Z) . If we write the total magnetic flux density in the source free region $h < Z < 0$ external to the half space as \vec{B}_s , derived from the potential ϕ_e , then

$$\phi_e = [A(\epsilon)e^{\lambda Z} + c(\epsilon)e^{-\lambda Z}]P(x, y) \quad (IV.1)$$

where $A(\epsilon)$ and $C(\epsilon)$ are independent of position, $P(X, Y)$ is a time dependent source function and λ is a wave number of the source-field. The term $C(\epsilon)$ in (IV.1) represents flux due to the primary, or source field (going to zero infinitely far from the source, i.e. as $Z \rightarrow \infty$), and the term with $A(\epsilon)$ represents flux due to secondary, or induced field (going to zero as $Z \rightarrow -\infty$). At the interface between any two media the fields must satisfy the usual boundary conditions of electromagnetism:

- the tangential components of \vec{E} and \vec{H} must be continuous.
- normal component of \vec{B} must be continuous

$$\beta = A(\epsilon) / c(\epsilon)$$

β gives the relative amplitudes and phase difference of the induced and the inducing fields. Numerical methods can be used to obtain solutions:

given the distribution $\sigma(Z)$.

In case of induction in a uniform half space by a known harmonic external field $e^{i\omega t}$, (IV.1) becomes

$$\phi_e = (Ae^{\lambda Z} + ce^{-\lambda Z})e^{i\omega t}P \quad (IV.2)$$

when we measure the total field, we do so on the interface between the vacuum and the conductor, which is the plane $Z = 0$. On this plane, the source field \vec{B}_s is

$$\vec{B}_s = - \left[c \frac{\partial P}{\partial x}, c \frac{\partial P}{\partial y}, -\lambda c P \right] e^{i\omega t} \quad (IV.3)$$

and the total field \vec{B}_t on the same plane

$$\vec{B}_t = - \left[(c+A) \frac{\partial P}{\partial x}, (c+A) \frac{\partial P}{\partial y}, \lambda (A-c) P \right] e^{i\omega t} \quad (IV.4)$$

From eqns (IV.3) and (IV.4) it is clear that the effect of the induced field is to increase the horizontal components of the source field and to decrease the vertical component. When the product $\sigma\mu\omega$ is very large compared with λ , it is found that $A \approx C$. In this limiting case

$$\vec{B}_t = - \left[2c \frac{\partial P}{\partial x}, 2c \frac{\partial P}{\partial y}, 0 \right] e^{i\omega t}$$

That is, in the limit of a uniform highly conducting half space and a high frequency source field the total magnetic field on the surface of the half space has zero vertical components and has horizontal component exactly twice the intensity of those of the source field. In cases other than this high-conductivity high-frequency limit the vertical component of the total field will be non-zero but less than that of the

source field, and the horizontal component will be greater than those of the source field, but by a factor of less than 2.

We can quantify these remarks in terms of the relation $\beta (= A(t)/C(t))$ and $\alpha = \pi \omega / \lambda^2$, a measure of the importance of induction effects. The table given below lists values of α and the corresponding values,

$\beta \backslash \alpha$	0.01	0.25	1.0	4.0	25	100
Modulus	0.0025	0.065	0.22	0.48	0.75	0.87
Argument (degree)	90	77	66	39	16	8

of modulus of β and its argument. A large value of α gives very strong induction effects, the induced horizontal field being almost as large as the inducing field and the phase difference between the two fields approaching zero. In the limit of high α the equations reduce to ordinary skin-depth formulas for good conductors. When α is small, the phase difference between the inducing and induced field approaches 90° , and the magnitude of the induced field is very small.

Analytical Techniques

There are several techniques to delineate the anomalous conducting zones with array data. Three of those which are presently in wide use are discussed here. First one is a simple stack plotting of the magnetic records of a sub-storm. Second one is through determination of transfer functions or Parkinson's vectors. The third method is based on the contour maps of Fourier amplitude and phase. Stacked magnetograms are extremely useful in qualitative interpretation. We have seen that

over a uniform half space, the vertical component of the field is very small and zero in case of highly conducting layers. Thus local anomalies, by perturbing the direction of flow of internal currents show up strongly in the Z-field. Though, such a perturbation effects X, and Y variations also, but there the normal field being large, the change is not distinct. Furthermore, as the sign of Z reverses on the two sides of a conducting zone, the Z-anomalies also help to locate the lateral extent of conductors. Combining the X,Y and Z anomalies one can easily identify the depth and extent of a conductor. The only limitation of this approach is that the analysis is done in time domain.

The second approach of plotting Parkinson's vector or its variant transfer functions can be appreciated by looking at Z/H ratio near a conductivity contrast. In areas where there is no lateral contrast in conductivity, the Z/H ratio will be very small and will have same value for all directions of polarisation of the source. On the contrary, near lateral contrasts, the Z/H ratio will be significantly non-zero and will be critically dependent on source field polarisation in relation to the strike of the sub-surface contrast. Because of this property of theirs, the Parkinson's vectors when displayed on maps of an array of observational points, clearly identify the location and trends of sub-surface anomalies. Later attempts to make the analysis more quantitative and amenable to model calculations resulted in the introduction of transfer functions. Transfer functions pair (A,B) commonly relate Z-variations to H- and D-variations, i.e.

$$Z(t) = A(t) H(t) + B(t) D(t) + E(t) \quad (IV.5)$$

f under brackets indicates the frequency dependence of the transfer functions. $\epsilon(f)$ is a measure of misfit and is minimised to obtain best values of A and B through a method that is discussed in the following section. Once A and B are determined the induction vector can be estimated from the formulae $\sqrt{A^2 + B^2}$. As A and B both have in-phase and quadrature component, the computed Parkinson's arrow too have real and quadrature parts.

The third method is based on the use of Fourier transforms. The usual Fourier series expansion of a discrete data set d_k with $k = 0, 1, \dots, N$, is

$$d_k = \frac{1}{2} a_0 + \sum_{j=1}^N \left(a_j \cos \frac{2\pi j}{N} k + b_j \sin \frac{2\pi j}{N} k \right)$$

or if we write,

$$\begin{aligned} \omega_j &= \frac{2\pi j}{N} \\ c_j &= \sqrt{a_j^2 + b_j^2} \\ \phi_j &= \tan^{-1} b_j/a_j \end{aligned}$$

we have

$$d_k = \frac{1}{2} a_0 + \sum_{j=1}^N c_j \cos(\omega_j k - \phi_j)$$

where a_j and b_j are Fourier Sine the Cosine coefficients, c_j is the Fourier amplitude and ϕ_j is the phase. Note that a more positive phase here represents a shift in wave form to a later time; the reverse convention is also used by some authors. The equivalent pairs of quantities a_j and b_j ; c_j and ϕ_j are calculated by applying a Fourier transform to the data set d_k .

Fourier amplitudes and phases are calculated for all the three elements M, D & Z. The Fourier transforms of the data sets d_k are found by the use of fast Fourier transform sub-routine. Maps across the array of Z, X and Y or Z, H and D at various periods have become the most common and most useful method of presenting data from an array. Fourier maps prepared for different polarisation of the source fields have proved extremely useful in delineating the trends of conductors.

Estimation of Transfer Functions

We wish to find the best fit for each station to the equation

$$Z = AH + BD$$

and thus obtain A & B. For this we minimise the residual

$$\epsilon = Z - AH - BD$$

Remember Z, H, D are Fourier amplitudes and A and B are functions of frequency. The least square estimate of A and B is their value that minimises

$$\sum_{r=1}^n \epsilon_r \epsilon_r^* = \sum_{r=1}^n (Z_r - AH_r - BD_r)(Z_r^* - A^*H_r^* - B^*D_r^*)$$

*signifies complex conjugate. The variable r runs over the n - different estimates of Z, H and D that are used to find A and B.

Minimising the residual squared $\sum \epsilon_r \epsilon_r^*$ with respect to the real and imaginary parts of A and B, we get

$$\sum_{r=1}^n H_r (Z_r^* - A^*H_r^* - B^*D_r^*) = P - A^*X - B^*Y$$

$$\sum_{r=1}^n D_r (Z_r^* - A^*H_r^* - B^*D_r^*) = Q - A^*X^* - B^*Y$$

$$\begin{aligned} \text{where } N &= \sum_{r=1}^n H_r H_r^* & P &= \sum_{r=1}^n H_r Z_r^* \\ W &= \sum_{r=1}^n D_r D_r^* & Q &= \sum_{r=1}^n D_r Z_r^* \\ X &= \sum_{r=1}^n H_r D_r^* \\ \therefore A &= \frac{P^* W - Q^* X^*}{N W - X X^*} ; & B &= \frac{Q^* N - P^* X}{N W - X X^*} \end{aligned}$$

Location of Conductor (Quantitative)

Once a conductor has been located either ^{known} Parkinson vector plots or through the Fourier amplitude phase contours, its exact geometry is determined through numerical modelling. One such method is the method suggested by Jones and Pascoe (Geophys. Journ Roy. Astron. Soc., Vol. 24, 1971, pp 3-30). The formalism is the two-dimensional structures. Assume that the conductivity is independent of the X-coordinate (i.e. $\partial/\partial x = 0$) and the Maxwell's equation (neglecting displacement current)

$$\nabla \times \vec{H} = 4\pi\sigma \vec{E}$$

$$\text{and } \nabla \times \vec{E} = -i\omega \vec{H}$$

reduce to

$$\frac{\partial H_z}{\partial y} - \frac{\partial H_y}{\partial z} = 4\pi\sigma E_x \quad (V.1)$$

$$\frac{\partial H_x}{\partial z} = 4\pi\sigma E_y \quad (V.2)$$

$$-\frac{\partial H_x}{\partial y} = 4\pi\sigma E_z \quad (V.3)$$

$$\frac{\partial E_z}{\partial y} - \frac{\partial E_y}{\partial z} = i\omega H_x \quad (V.4)$$

$$\frac{\partial E_x}{\partial z} = i\omega H_y \quad (V.5)$$

$$-\frac{\partial E_x}{\partial y} = i\omega H_z \quad (V.6)$$

(V.1), (V.5) & (V.6) involve only E_x , H_y and H_z

(V.2), (V.3) & (V.4) involve only H_x , E_y and E_z

The former is called E-polarisation and the latter H-polarisation case depending on the direction of the inducing field E_x or H_x parallel to the strike of the conductor. The physical interpretation of E-polarisation case is that the current flow is parallel to the strike, whereas in H-polarisation case, the current flow is perpendicular to the strike of the conductor. For both these polarisation cases, the equation to be solved in various regions are identical and are given as:

$$\begin{aligned} &\text{E - polarisation} \\ &\frac{\partial^2 E_x}{\partial y^2} + \frac{\partial^2 E_x}{\partial z^2} = i\eta^2 E_x \quad (V.7) \end{aligned}$$

$$\begin{aligned} &\text{H - polarisation} \\ &\frac{\partial^2 H_x}{\partial y^2} + \frac{\partial^2 H_x}{\partial z^2} = i\eta^2 H_x \quad (V.8) \end{aligned}$$

with $\eta^2 = 4\pi\sigma\omega$. These equations must be solved in each region with appropriate boundary conditions and appropriate conductivity (σ). The sub-surface region is divided into a rectangular mesh

grids. Each grid is given an appropriate conductivity value. Finite difference equations for each mesh of grid points covering the entire region are solved by Gauss-Seidel method. The actual estimation of conductivity is made by making a best fit to the observed surface anomalies.

SUMMARY

Magnetotellurics is a method which has been gaining increasing acceptance because of its simplicity, its ability to carry out surveys rapidly, and the depth penetration potential since the source is at a large distance. The method is particularly useful when operated as a mapping device, due mainly for the very high lateral resolution it has. The source being effectively at infinity, the method has the capacity of greater depth penetration than any comparable electromagnetic method which is limited by distance between transmitter and receiver.

Basically, the ratio of the horizontal electric field (E) in the ground to the orthogonal horizontal magnetic field (H), is measured at a number of frequencies. The ratio of E/H, which has dimension of impedance, is calculated as a function of frequency. This parameter is used to calculate the resistivity of earth as a function of depth. Operationally, the whole approach is quite simple, in the sense that depth sounding is conducted by making measurements at only one location.

The process can be described as the interaction of an electromagnetic wave with the earth. In the process fluctuating magnetic field induce electric currents inside the earth. The incident, horizontal magnetic field, is roughly doubled at the surface of the earth, and it is uniform in the absence of lateral contrasts in resistivity. The electric field, on the other hand, is directly dependent upon the earth's resistivity structure.

Depth of sounding can be roughly related to the frequency by use of the skin depth, defined as:

$$\delta = \sqrt{\frac{2\rho}{\pi f \mu}} = \sqrt{\frac{2}{\sigma \mu \omega}} \quad \text{where;}$$

δ = skin depth in meters

f = frequency in hertz

$\rho = \left(\frac{1}{\sigma}\right)$ = resistivity in ohm - meters.

μ = permeability in henry/meters.

The apparent resistivity can be determined simply from the measured impedance [E/H] through the relationship:

$$\rho_a = \frac{1.26 \times 10^5 (E/H)^2}{f} \quad ; \text{ when } E \text{ is in Volts/meter and}$$

H in amp. turn/meter. Frequency, however, the conductivity structure of the earth, can not be truly represented by a layered - media approximation. For instance, a mineral deposit may create zones of conductivity contrasts of complex shape. In such a situation E and H are not orthogonal and their ratio becomes a function of plane of polarization of the incident wave. This happens so because the induced currents preferentially tend to flow into a medium of high conductivity. Therefore, current induced by the geomagnetic field may flow in a direction controlled by the local geology rather than in a perpendicular direction to the magnetic field source component, as expected when no lateral resistivity contrast is present. Complications now arise because the measured impedance at the surface of the earth is no longer independent of either the orientation of the orthogonal fields measured or the polarisation of the incoming source field. Modelling becomes difficult in such situations.

Introduction

Magnetotelluric prospecting is a relatively new method of geophysical prospecting, though the electric and magnetic field it employs have long been observed. More than a century ago, it was recognised that a correlation existed between the variations in telluric currents and the geomagnetic field. The major development came in early 1950's with the work of Cajniard in France and of Tikhonov in the U.S.S.R. In 1953, Cajniard published a paper in Geophysics (vol. 18, pp. 605-635) in which he gave a quantitative description of the relationship between electric field and magnetic fields at the surface of a horizontally layered earth. Soon it was realized that the impedance is not always scalar and in many of the solutions the E/H ratio depends on the direction of H and E. In reality, except for one dimensional case, the impedance is a tensor and the relationship between the electric field (E) and magnetic field (H) at any given frequency is expressed as:

$$\begin{pmatrix} E_x \\ E_y \end{pmatrix} = \begin{pmatrix} Z_{xx} & Z_{xy} \\ Z_{yx} & Z_{yy} \end{pmatrix} \begin{pmatrix} H_x \\ H_y \end{pmatrix}$$

The expression is written in Cartesian coordinate system. E_x , E_y are the horizontal component of the electric field E in two orthogonal directions. H_x , H_y are the component of the magnetic field in the same two directions. Elements of the impedance tensor are the Z's. The Z - tensor is a function of frequency and depends upon the conductivity of the earth in its surrounding areas. If the horizontal wavelengths of the incident fields are sufficiently long, Z will be independent of time and source polarization. Therefore, Z can be a useful measure of the conductivity structure of the earth, and in fact it has been used to develop the model of internal structures in resource locations.

The magnetotelluric study can conveniently be divided into three parts: data acquisition, estimation of elements of Z and finally modelling the geoelectrical structure of the subsurface layers. A more ^{recent} development is the use of the depth conductivity profile so obtained to find the physical and chemical state of the interior combining the measured conductivity with properties of rocks determined from laboratory studies.

In the presentation we first consider the relationship between resistivity (inverse of conductivity) of the earth's interior and the impedance as observed on the earth's surface. This will give an understanding of how to design the observational set up and above all how the magnetotelluric method works. After this, we will have a brief description of the MT unit. Once the measuring system are outlined, the procedure adopted to estimate Z-tensor and modelling of the structure of the surveyed region will be taken up.

Theoretical Basis of the Magnetotelluric Method

We shall be first considering one - dimensional cases and then shall take up two and three dimensional structures. In the one dimensional case, we start with homogeneous half space.

Homogeneous Half Space Model

This is the simplest of all possible models. Here the earth is considered to be homogeneous and isotropic having conductivity σ , permittivity ϵ , and permeability μ . Assuming time variations as $e^{j\omega t}$, the Maxwell's equations in the medium can be written as:

..5..

$$\nabla \times \vec{E} = -j\omega\mu\vec{H} \quad (1.1)$$

$$\nabla \times \vec{H} = (\sigma + j\omega\epsilon)\vec{E} \quad (1.2)$$

$$\nabla \cdot \vec{H} = 0 \quad (1.3)$$

$$\nabla \cdot \vec{E} = 0 \quad (1.4)$$

The first term $\sigma\vec{E}$ on the right side of (1.2) represents conduction currents, while the second term $j\omega\epsilon\vec{E}$ represents displacement currents. The ratio of the two types of currents is

$$\frac{\omega\epsilon}{\sigma} = \frac{2\pi \cdot \text{P.P.} \cdot 10^{-9}}{36\pi} \approx \frac{1}{2} \frac{\rho}{\tau} \times 10^{-10}$$

For ϵ , we have used permittivity of free space = $10^{-9}/36\pi$ F/M

In the above equation, τ is frequency and τ is period of the electromagnetic field. The normal range of periods used in magnetotelluric sounding varies from 0.01 sec to ≈ 1000 sec, and the resistivities encountered in the earth range from 1 to 1000 ohm-m. Therefore it is clear that the displacement currents can be neglected when considering the application of the MT methods. This in turn means that we are dealing with a pure diffusion process; i.e., a quasi-stationary field which is described by system of equations:

$$\nabla \times \vec{E} = -j\omega\mu\vec{H}$$

$$\nabla \times \vec{H} = \sigma\vec{E}$$

$$\nabla \cdot \vec{H} = 0$$

$$\nabla \cdot \vec{E} = 0$$

Coming back to the general case, we can write

$$\begin{aligned} \nabla \times \nabla \times \vec{E} &= -j\omega\mu (\nabla \times \vec{H}) \\ &= -j\omega\mu (\sigma + j\omega\epsilon) \vec{E} \end{aligned}$$

..6..

and

$$\begin{aligned} \nabla \times \nabla \times \vec{E} &= (\sigma + j\omega\epsilon) \nabla \times \vec{E} \\ &= -j\omega\mu (\sigma + j\omega\epsilon) \vec{H} \end{aligned}$$

$$\left[\text{Recall } \nabla \times \nabla \times \vec{A} = \nabla (\nabla \cdot \vec{A}) - \nabla^2 \vec{A} \right]$$

Since, except at the boundaries $\nabla \cdot \vec{A} = 0$; we get

$$\nabla^2 \vec{E} = j\omega\mu (\sigma + j\omega\epsilon) \vec{E}$$

$$\text{and } \nabla^2 \vec{H} = j\omega\mu (\sigma + j\omega\epsilon) \vec{H}$$

Putting

$$\gamma^2 = j\omega\mu\sigma - \omega^2\mu\epsilon \quad (1.5)$$

the equations reduce to vector Helmholtz equation :

$$\nabla^2 \vec{E} = \gamma^2 \vec{E}$$

$$\nabla^2 \vec{H} = \gamma^2 \vec{H}$$

In rectangular cartesian coordinates, this vector equation separates, so that each of the components of \vec{E} and \vec{H} fields satisfies the scalar Helmholtz equation. Elementary solutions of this equation are of the form

$$A e^{-(\gamma_x x + \gamma_y y + \gamma_z z)}$$

$$\text{where } \gamma^2 = \gamma_x^2 + \gamma_y^2 + \gamma_z^2 = j\omega\mu\sigma - \omega^2\mu\epsilon \quad (1.6)$$

The general equation is obtained by taking the sum of such elementary solutions with different values of A , γ_x , γ_y & γ_z . If the coordinate axes are aligned such that positive z is down, and the direction of propagation is in the $x-z$ plane, the elementary solution is of the form

$$A e^{-\gamma_x x - \gamma_z z} ; \gamma_x^2 + \gamma_z^2 = \gamma^2 \quad (1.7)$$

..7..

Any homogeneous plane wave can be separated into TE (horizontal E field only) or TM (horizontal H field only) modes, and since the equations are linear with respect to the fields the two modes can be treated separately.

For the TE mode

$$E_x = E_z = 0$$

From eqn (I.1)

$$\nabla \times \vec{E} = -j\omega\mu\vec{H}$$

$$\begin{vmatrix} \vec{i} & \vec{j} & \vec{k} \\ \frac{\partial}{\partial x} & \frac{\partial}{\partial y} & \frac{\partial}{\partial z} \\ 0 & E_y & 0 \end{vmatrix} = -j\omega\mu (H_x\vec{i} + H_y\vec{j} + H_z\vec{k})$$

$$\text{or, } -\vec{i} \frac{\partial E_y}{\partial z} + \vec{k} \frac{\partial E_y}{\partial x} = -j\omega\mu (H_x\vec{i} + H_y\vec{j} + H_z\vec{k})$$

Thus

$$\frac{\partial E_y}{\partial z} = j\omega\mu H_x$$

$$\frac{\partial E_y}{\partial x} = -j\omega\mu H_z$$

i.e.,

$$-\gamma_z E_y = j\omega\mu H_x$$

$$-\gamma_x E_y = -j\omega\mu H_z$$

$$H_y = 0$$

In particular

$$Z_{TE} = \frac{-E_y}{H_x} = \frac{j\omega\mu}{\gamma_z}$$

(I.8)

..8..

For the TM mode

$$H_x = H_z = 0$$

Eqn (I.2) gives

$$-\frac{\partial H_y}{\partial z} \vec{i} + \frac{\partial H_y}{\partial x} \vec{k} = (\sigma + j\omega\epsilon) (E_x\vec{i} + E_y\vec{j} + E_z\vec{k})$$

$$\text{hence } \gamma_z H_y = (\sigma + j\omega\epsilon) E_x$$

$$-\gamma_x H_y = (\sigma + j\omega\epsilon) E_z$$

$$0 = E_y$$

and

$$Z_{TM} = \frac{E_x}{H_y} = \frac{\gamma_z}{\sigma + j\omega\epsilon} = \frac{j\omega\mu\gamma_z}{\gamma^2} \quad (I.9)$$

In the MT applications

$$\omega\epsilon \ll \sigma$$

and

$$\gamma^2 = j\omega\mu\sigma \quad (I.10)$$

The magnetotelluric method is dependent on the ability to deduce the earth parameters from the surface impedance function, requiring that the source effect be either known or negligible. Theoretical treatments of the source effect for 1-dimensional geometry point out that limitations must be placed on the horizontal derivatives of the source field in order to reduce its effect in the surface impedance. For a one-dimensional earth, any lateral components in the propagation vectors γ are due to γ_x and γ_y . Therefore, in order to have an effectively normally incident plane wave, the source field should have

$$|\gamma_x| \text{ and } |\gamma_y| \ll \gamma$$

..9..

$$\text{i.e. } \gamma_z = \gamma = \sqrt{j\omega\mu\sigma} \quad (1.11)$$

under this condition

$$Z_{TM} = \frac{j\omega\mu}{\gamma_z}$$

i.e.

$$\begin{aligned} Z_{TE} &= Z_{TM} = \frac{j\omega\mu}{\gamma} = \frac{j\omega\mu}{\sqrt{j\omega\mu\sigma}} \\ &= \sqrt{\frac{j\omega\mu}{\sigma}} \end{aligned} \quad (1.12)$$

This implies that the impedance is independent of the polarization of the elementary solution. Thus, any general solution made up of elementary solutions satisfying the conditions of equation (1.11) will give a scalar impedance

$$Z = \sqrt{\frac{j\omega\mu}{\sigma}} \quad (1.13)$$

which will relate any horizontal component of the total H field to the orthogonal component of E field. It is now convenient to define a parameter, δ , called skin depth, defined by

$$\delta = \sqrt{\frac{2}{\omega\mu\sigma}} \quad (1.14)$$

$$\begin{aligned} \text{Then } e^{-\gamma_z z} &= e^{-\sqrt{2}j} \quad \text{when } z = \delta \\ &= e^{-(1+j)} = e^{-1} \cdot e^{-j} \end{aligned}$$

..10..

Thus δ is a measure of the depth at which the field will have been attenuated to $1/e$ of its surface value

Note:

$$\begin{aligned} \gamma_z &= \sqrt{j\omega\mu\sigma} = \frac{1+j}{\delta} \\ \left(\frac{1+j}{\delta}\right)^2 &= 2j\omega\mu\sigma = j\omega\mu\sigma = \gamma_z^2 \\ e^{-\gamma_z z} &= e^{-(1+j)z/\delta} \\ &= \underbrace{e^{-z/\delta}}_{\text{exponentially decreasing}} \cdot \underbrace{e^{-jz/\delta}}_{\text{oscillatory}} \end{aligned}$$

The term $e^{-z/\delta}$ represents a decrease in field strength by a factor e^{-1} when $z = \delta$. The term $e^{-jz/\delta}$ represents a change of phase with depth. It is obvious that when $z = 2\pi\delta$, the phase of the field components change by 2π . This is the reason that $2\pi\delta$ is called the wavelength.]

Coming back to equation (1.13)

$$\begin{aligned} Z &= \sqrt{\frac{j\omega\mu}{\sigma}} \\ [\text{Recall: } e^{j\pi/2} &= j \quad \therefore e^{j\pi/4} = \sqrt{j}] \\ \text{i.e. } Z &= \sqrt{\frac{\omega\mu}{\sigma}} \cdot e^{j\pi/4} \end{aligned} \quad (1.15)$$

Thus for a uniform half space Z does not depend upon the thickness z of the conductor. A phase difference of $\pi/4$ introduced between the electric and magnetic fields. The electric field is shifted in phase by -45° with respect to magnetic field. Magnitude of impedance Z depends upon the conductivity, but the phase is independent of the same. Further as δ is dependent on ω , the depth of investigation changes with period of oscillation. When period increases, δ increases, the currents penetrate deeper increasing the depth of the region investigated.

Horizontally Layered Model

The next method we take is one in which the earth is represented by a set of horizontal layers, each with a different conductivity. The layers characteristics are σ_i, d_i (Fig. 1). This is usually known as Coignard model since this is the one that he considered in his classic paper. Let us take the number of layers to be N . The elementary solution in each layer for \vec{E} or \vec{H} will have the form

$$(A_i e^{-\gamma_{2i} z} + B_i e^{+\gamma_{2i} z}) e^{-\gamma_{1i} x} \quad (1.16)$$

where

$$\gamma_{1i}^2 + \gamma_{2i}^2 = \gamma_i^2 = j\omega\mu\sigma_i$$

Requiring that tangential electric and magnetic field be continuous at each boundary, one finds that the impedance Z_i looking down from the top of the i^{th} layer is given by

$$Z_i = Z_{oi} \frac{1 - R_i e^{-2\gamma_{2i} d_i}}{1 + R_i e^{-2\gamma_{2i} d_i}} \quad i = 1, 2, \dots, N-1 \quad (1.17)$$

and $Z_N = Z_{oN}$

For the N^{th} layer $B_N = 0$. In equation (1.17) d_i is the thickness of the i^{th} layer, R_i is reflection coefficient defined by

$$R_i = \frac{Z_{oi} - Z_{i+1}}{Z_{oi} + Z_{i+1}} \quad ; \quad i = 1, 2, \dots, N-1 \quad (1.18)$$

In both (1.17) and (1.18) Z_{oi} is the characteristic impedance of the i^{th} layer.

One may start with the bottom layer and work up computing R_i and Z_i using recursion equation (1.17) and (1.18) until Z_1 the surface impedance, is obtained. Recall from (1.13)

$$\sigma = \frac{\omega\mu}{|Z|^2}$$

correspondingly, for a layered earth, it is customary to define an apparent conductivity $\sigma_a(\omega)$ or apparent resistivity $\rho_a(\omega)$ by

$$\sigma_a(\omega) = \frac{\omega\mu}{|Z_1(\omega)|^2} = \frac{1}{\rho_a(\omega)} \quad (1.19)$$

Some sample curves of apparent resistivity versus frequency for two models are shown in Figs. 2 and 3. For high frequencies, $\sigma_a = \sigma$, and for low frequencies, $\sigma_a = \sigma_N$. Qualitatively, it appears that $\sigma_a(\omega)$ is a "smoothened out" version of $\sigma(z)$ with frequency ω being inversely related to depth z .

Although, the calculation of $Z_1(\omega)$ is simple when $\sigma(z)$ for a layered earth is given, the reverse procedure of finding $\sigma(z)$ given $Z_1(\omega)$ is not easy. The latter, is a non-linear problem. This aspect will be discussed later.

II Two and Three Dimensional Cases

A structure is two-dimensional when the conductivity besides depending on z , also depends upon one of the two horizontal axes x or y . When it depends on all the three (x , y and z), the structure is called three dimensional. The expression for scalar impedance deduced in the last section is not valid in case of two- and three-dimensional structures. Appropriate relationship will now be developed.

For the two-dimensional configuration, let us assume that the conductivity depends upon x and z and is independent of y . y axis, is then called the direction of strike.

Z_{TE} and Z_{TM} for 2-D Models

Consider again Maxwell's equation (I.1) - (I.4) and assume σ is a function of x and z . The difference from 1-D case now is that we should consider instead of (I.4), the equation

$$(\nabla \cdot \sigma \vec{E}) = 0 \quad (II.1)$$

Let us again assume that the horizontal wavelengths of the incident fields are long compared to a skin depth. Everything thus remains uniform in y - direction and we have

$$\nabla \times \vec{E} = -j\omega\mu \vec{H} \quad (I.1)$$

$$\nabla \times \vec{H} = \sigma \vec{E} \quad (I.2)$$

$$\nabla \cdot \vec{H} = 0 \quad (I.3)$$

$$\nabla \cdot \sigma \vec{E} = 0 \quad (II.1)$$

From I.1

$$-\frac{\partial E_y}{\partial z} = -j\omega\mu H_x \quad (II.2)$$

$$\frac{\partial E_x}{\partial z} - \frac{\partial E_z}{\partial x} = -j\omega\mu H_y \quad (II.3)$$

$$\frac{\partial E_y}{\partial x} = j\omega\mu H_z \quad (II.4)$$

From I.2

$$-\frac{\partial H_y}{\partial z} = \sigma E_x \quad (II.5)$$

$$\frac{\partial H_x}{\partial z} - \frac{\partial H_z}{\partial x} = \sigma E_y \quad (II.6)$$

$$\frac{\partial H_y}{\partial x} = \sigma E_z \quad (II.7)$$

From I.3

$$\frac{\partial H_x}{\partial z} + \frac{\partial H_z}{\partial x} = 0 \quad (II.8)$$

From II.1

$$\frac{\partial(\sigma E_x)}{\partial x} + \frac{\partial(\sigma E_z)}{\partial z} = 0 \quad (II.9)$$

They can be grouped into two pairs:

$$\frac{\partial E_y}{\partial z} = j\omega\mu H_x$$

$$\frac{\partial E_x}{\partial z} - \frac{\partial E_z}{\partial x} = -j\omega\mu H_y$$

$$\frac{\partial E_y}{\partial x} = j\omega\mu H_z$$

$$-\frac{\partial H_y}{\partial z} = \sigma E_x$$

$$\frac{\partial H_x}{\partial z} - \frac{\partial H_z}{\partial x} = \sigma E_y$$

$$\frac{\partial H_y}{\partial x} = \sigma E_z$$

$$\frac{\partial H_x}{\partial z} + \frac{\partial H_z}{\partial x} = 0$$

$$\frac{\partial(\sigma E_x)}{\partial x} + \frac{\partial(\sigma E_z)}{\partial z} = 0$$

The two groups of equations are decoupled. One set contains only E_y , H_x and H_z ; while the other set contains E_x , E_z and H_y . The mode involving E_y , H_x and H_z is usually called TE or E parallel mode. Since the E field is horizontal and parallel to the strike. The mode involving E_x , E_z and H_y is called TM or E - perpendicular mode since the magnetic field is horizontal and the electric field is perpendicular to the strike. There are no variations in the model parameters, in the direction of strike, the y -axis, in this case.

Thus, for a two - dimensional model two impedances are required to define the relationship between E and H fields: i.e.

$$Z_{TE} = \frac{-E_y}{H_x} ;$$

$$\text{and } Z_{TM} = \frac{E_x}{H_y}$$

Exact solutions for $Z_{TE}(\omega, x)$ and $Z_{TM}(\omega, x)$ in terms of (x, z) are not tractable analytically. In general numerical methods are used. These are strongly dependent on grid size.

Z for 2-D in a general co-ordinate system

The TE- and TM modes decouple when one of the horizontal axes is aligned to the direction of strike. It will be useful to obtain a relationship in a coordinate system which is arbitrarily oriented. Suppose the $X' - Y'$ coordinate system as shown in Fig. 4 aligned with the strike; so that

$$E_{x'} = Z_{TM} H_{y'} \quad (11.10)$$

$$\text{and } E_{y'} = -Z_{TE} H_{x'} \quad (11.11)$$

Suppose the $X-Y$ coordinate system is oriented at an angle θ with respect to the $X'-Y'$ system as shown in Fig. 4. In that case

$$E_x = E_{x'} \cos \theta + E_{y'} \sin \theta \quad (11.12)$$

$$E_y = -E_{x'} \sin \theta + E_{y'} \cos \theta \quad (11.13)$$

$$\text{and } H_x = H_{x'} \cos \theta + H_{y'} \sin \theta \quad (11.14)$$

$$H_y = -H_{x'} \sin \theta + H_{y'} \cos \theta \quad (11.15)$$

Alternatively

$$H_{x'} = H_x \cos \theta - H_y \sin \theta \quad (11.16)$$

$$H_{y'} = H_x \sin \theta + H_y \cos \theta \quad (11.17)$$

Now, we can write

$$\begin{aligned} E_x &= E_{x'} \cos \theta + E_{y'} \sin \theta \\ &= Z_{TM} H_{y'} \cos \theta - Z_{TE} H_{x'} \sin \theta \\ &= Z_{TM} (H_x \sin \theta + H_y \cos \theta) \cos \theta - Z_{TE} (H_x \cos \theta - H_y \sin \theta) \sin \theta \\ &= H_x [(Z_{TM} - Z_{TE}) \sin \theta \cos \theta] + H_y [Z_{TM} \cos^2 \theta + Z_{TE} \sin^2 \theta] \end{aligned}$$

Thus, if one defines:

$$E_x = Z_{xx} H_x + Z_{xy} H_y$$

$$\text{then } Z_{xx} = \frac{Z_{TM} - Z_{TE}}{2} \sin 2\theta$$

$$Z_{xy} = Z_{TM} \cos^2 \theta + Z_{TE} \sin^2 \theta$$

$$= \left(\frac{Z_{TM} + Z_{TE}}{2} \right) + \left(\frac{Z_{TM} - Z_{TE}}{2} \right) \cos 2\theta$$

Similarly for the other components, one obtains:

$$Z_{yx} = - \left(\frac{Z_{TM} + Z_{TE}}{2} \right) + \left(\frac{Z_{TM} - Z_{TE}}{2} \right) \cos 2\theta$$

$$Z_{yy} = \frac{Z_{TE} - Z_{TM}}{2} \sin^2 \theta$$

In summary:

$$\begin{pmatrix} E_x \\ E_y \end{pmatrix} = \begin{pmatrix} Z_1 \sin 2\theta & Z_2 + Z_1 \cos 2\theta \\ -Z_2 + Z_1 \cos 2\theta & -Z_1 \sin 2\theta \end{pmatrix} \begin{pmatrix} H_x \\ H_y \end{pmatrix} \quad (11.18)$$

$$\text{where } Z_1 = (Z_{TM} - Z_{TE})/2 \quad (11.19)$$

$$Z_2 = (Z_{TM} + Z_{TE})/2 \quad (11.20)$$

In general, then, for a two dimensional model, the tangential components of E and H are related by a rank two tensor impedance. The diagonal terms have opposite sign and they reduce to zero when the axes are aligned with the strike.

Three - Dimensional Case

Here σ is a function of all three coordinates x, y & z. The six field components are all coupled to each other, so it is not possible to separate the analysis into two distinct modes. A rank - two tensor impedance is still unique and stable, subject of course to the condition that the horizontal wavelengths of the incident fields are long compared to a skin depth in the earth.

For a three dimensional case, the elements Z-tensor trace ellipses in the complex plane as the measuring axes are rotated (Fig. 5). The ellipses degenerate to straight lines for the

two dimensional case. Also one notices that since the diagonal elements in 2-D case have no constant term, the straight line representing locii of Z_{xx} and Z_{yy} in the complex plane passes through the origin.

The solution of general 3-D case is difficult. For this reason, it is usually desirable to find one- dimensional or two-dimensional models that approximately fit measured data. It frequently happens that, over some limited frequency range, measured data looks almost two dimensional; i.e. Z - ellipses almost collapses to straight lines and the diagonal elements are almost negative of each other. This situation will occur whenever there exists a horizontal direction along which the conductivity cross-section is nearly constant for a distance of several skin depths. Whenever, such a situation exists, it is desirable to determine the approximate strike direction and to estimate the corresponding Z_{TE} and Z_{TM} for comparison with theoretical Z's from 2-D models.

There are several methods for finding the angle θ . One amongst these is to look for θ that maximises $\left[|Z_{xy}|^2 + |Z_{yx}|^2 \right]$ or minimises $\left[|Z_{xx}|^2 + |Z_{yy}|^2 \right]$. Having thus determined the principal axes, we should have some measure to test how two-dimensional the data is. There are two parameters that should be considered for this purpose. First, is the ratio of constant terms in diagonal and off diagonal elements of the Z-matrix.

$$\text{i.e. the ratio } \frac{Z'_{xx} + Z'_{yy}}{Z'_{xy} - Z'_{yx}}$$

Second is the ratio of the minor axis to the major axis of the $Z_0(\theta)$ ellipse. The magnitudes of both these ratios should be small compared to unity in order for the data to fit a two- dimensional model.

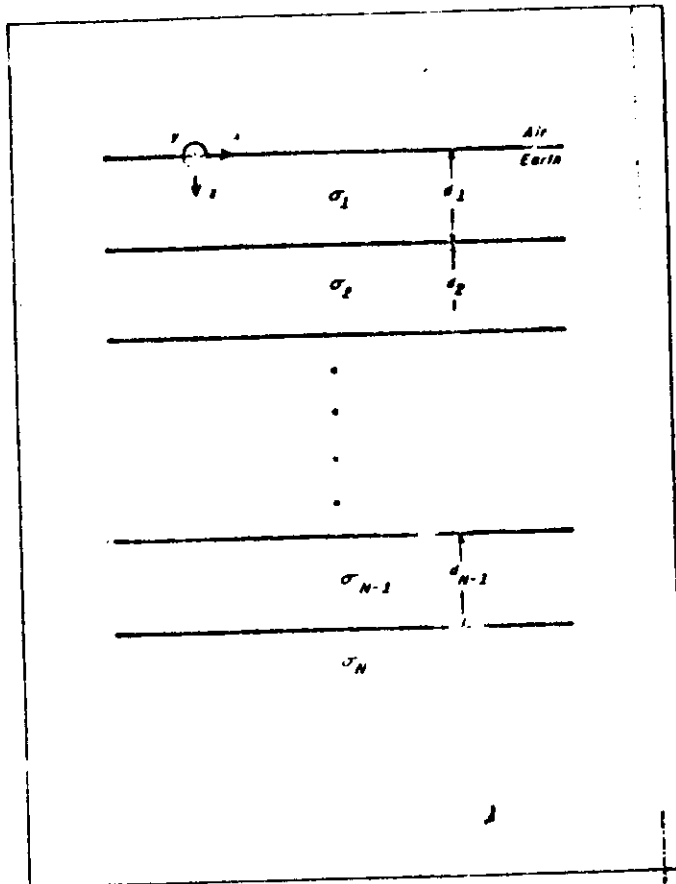


Fig. 1 Description of N Layer Model

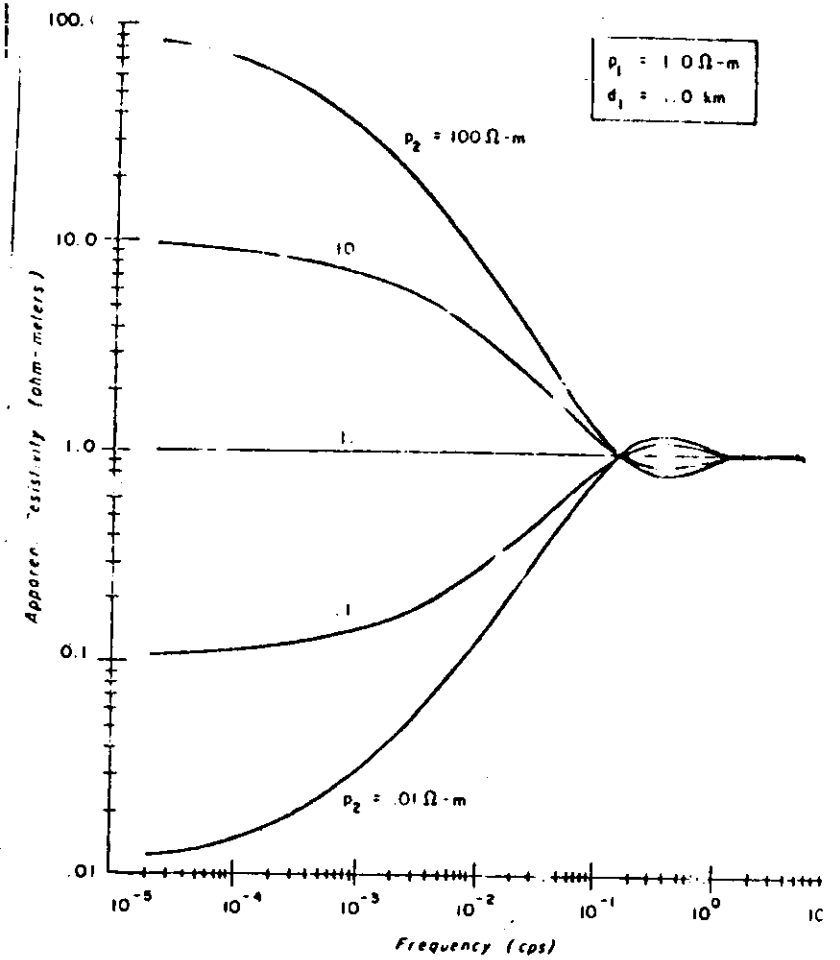


Fig. 2 Sample Two Layer Apparent Resistivity Curves

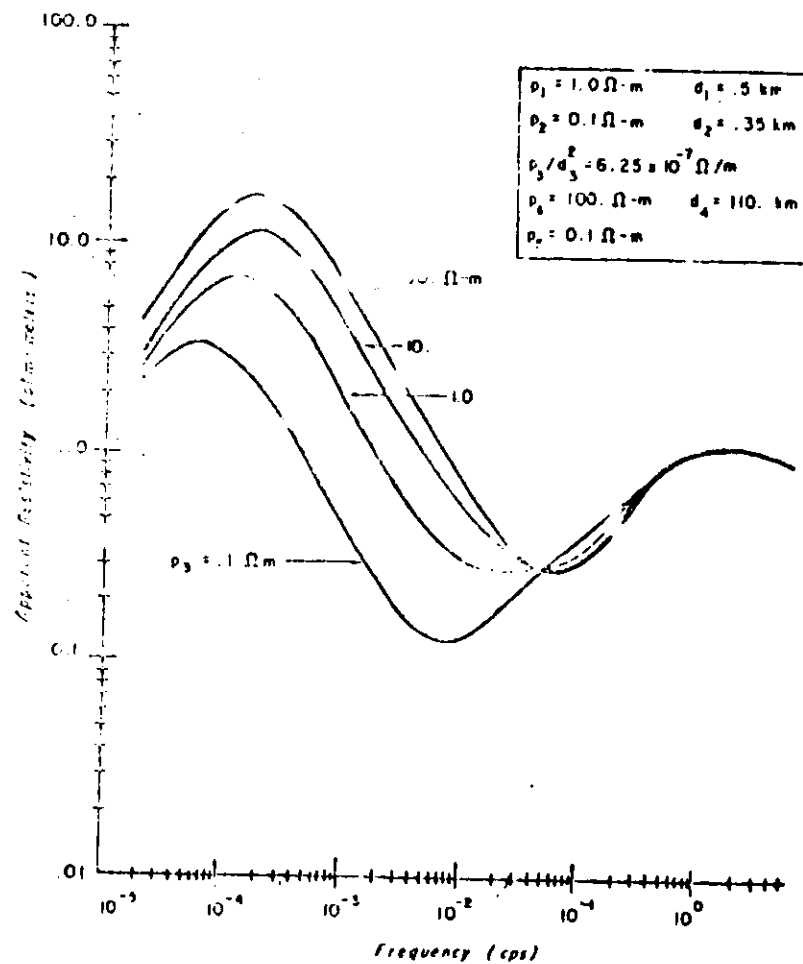


Fig. 3 Sample Five Layer Apparent Resistivity Curves

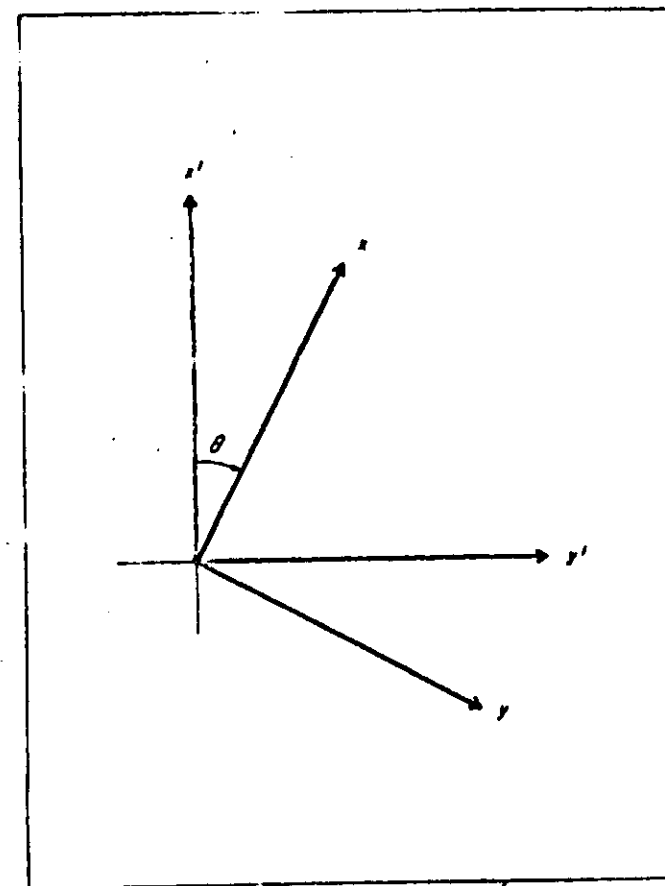


Fig. 4 Relative Orientation of $x'-y'$ and $x-y$ Coordinate Systems

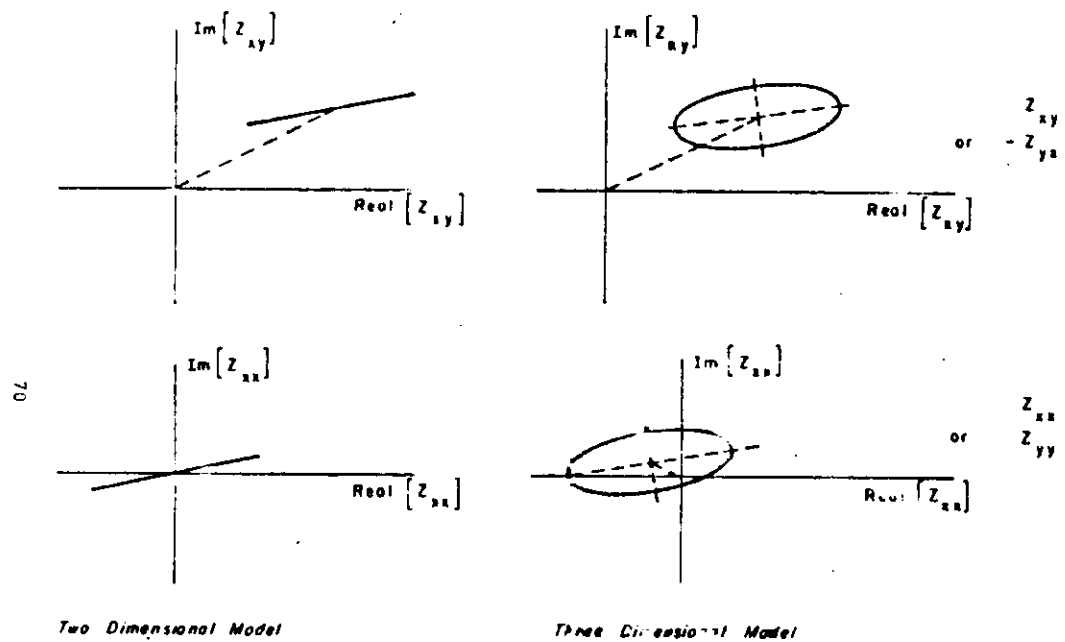


Fig. 5 Loci of Z_{ij} in the Complex Plane as the Measuring Axes are Rotated

Electromagnetic induction is presently being used extensively by geophysicists to study the earth's interior. To this end, geophysicists have developed various measuring techniques which can be used on land, off-shore, in the air and even inside the earth, in boreholes. Some of these systems are old but when correctly updated can still be useful. Other systems have recently been developed. The earth's field that is to be measured is often very small (1 μ V or less). This measurement is difficult because of the presence of various noises which can be larger than the desired signal (e.g. noise of the input amplifier, probes, interference noise, etc.) Important technical developments have recently been made concerning amplification of weak signals and these have led to the possibility of measuring accurately the telluric field.

Devices designed to measure the magnetic field or its components involve a large number of physical principles and this leads to a wide number of different sensors. The first measurements of the transient field were made with suspended magnet variometers and with induction sensors. These two kinds of devices still give valuable information thanks to some improvements such as the field feed-back. For absolute measurements it is better to use magnetic resonance devices. The use of this kind of device is compulsory when one needs to move the sensor quickly, as for example, when preparing a magnetic map from a boat or a plane. Finally, the fluxgate is a kind of directional magnetometer, light, compact, useful for various applications requiring neither high performance nor good stability with time.

In modern devices, when high frequency phenomena are to be studied,

the data is collected in digital form. This makes their processing easier. Some devices are equipped with microprocessor to process the data in real time, in the field.

Electric Probes

Measuring the variable potential difference which appears between two electrodes is not difficult at high frequencies, above 10 to 20 Hz for instance. The electronic industry supplies at present low-noise and high - input - impedance amplifiers, perfectly adapted to the measurement of a few microvolts. It is more or less the potential difference one can get by using telluric lines, a hundred meters long. In this case the nature of electrodes is not very important.

On the contrary, in the field of low or very low frequencies the measurement is much more difficult. Two electrodes buried in the earth form an electrical battery whose electromotive force varies with many factors such as temperature, dampness or physical composition of the earth. The smallest variation of one of these parameters leads to an interfering signal, often much greater than the potential difference to be measured. This brings the need of preferably impolarizable electrodes made of metal in contact with a solution of its own salts; the electromotive force of polarization does not disappear but it becomes much less important. The electrochemical reaction between the earth and the electrode are so complex that researches in order to improve the accuracy of the electric field determination are very often empirical.

One of the first electrodes made on this principle used the couple Ag-AgCl proposed by Fillard in 1967. It is still widely

used and is manufactured semi-industrially. One can also use combination of cadmium-chloride with Cadmium or Copper with copper-sulphate or one can use calomel electrode. With all these electrodes, it seems difficult to reduce the random drift below 2 or 3 $\mu\text{V hr}^{-1}$ even with buried electrodes. It is perhaps not necessary to have better performances. Indeed experience shows that the effect due to local distortion of the current lines flowing at shallow inhomogeneous layers of the earth or the topographic noise are more than the limit of instrumental noise already achieved.

Magnetic Sensors

Nuclear magnetic resonance or optical pumping devices measure the modulations of the total field independently of its direction. They are absolute sensors, for the measured signal (the gyromagnetic frequency) is linked to the magnetic field by nuclear or atomic parameters and does not depend on the experimental conditions. Such magnetometers, particularly those using free precession, have a long term stability much superior to other devices ~~and~~ having a comparable sensitivity. They are very good observatory sensors. Cancelling some components of the Earth's magnetic field, it is possible to use them as directional variometers. Conversely, it is possible to take advantage of their insensitivity in orientation, to take measurements on a wide scale. Nevertheless, they are not very useful for the study of the transient geomagnetic field as they can easily measure only ΔF . Components can only be obtained by using compensating coils of large size, which makes these sensors difficult

to handle in the field.

Suspended magnet variometers were the first devices used to study the transient magnetic field and are still widely used. They can be divided into two groups first, those for which the magnetic couple exerted on the magnet is compensated by a couple of different origin, for instance the torque of a wire. This principle is used in Askania variographs, in devices designed by Bobrov in 1971 and by Gough and Reitzel in 1967. This last one, cheap and easy to build, has allowed researchers, to use large arrays of magnetometers and thus measure the field simultaneously at a great number of stations. As the magnetic moment of this magnet and compensating torque vary with temperature according to different laws, such magnetometers have fairly large thermal drifts depending on the ambient thermal conditions. It is then necessary, either to control the device thermostatically, or to bury it, or to try to cancel the drift by that of another element, sensitive to temperature. The use of optical devices amplifying the rotation of the magnet makes these instruments difficult to handle and their photographic recording system does not permit easy data processing.

A second group includes variometers in which the variations of the natural field are compensated by those equal and opposite - of a field H^* -created near the magnet by an electronic feed-back system. The magnet is subjected only to the residual couple $M(H-H^*)$, extremely weak, and its direction in space is almost invariable. The small

rotations due to the field $H-H^*$ are measured with a very sensitive detector and they are used for producing the feedback field after amplification. In this type of variometers, the sensitivity is constant in the whole pass band. It gives an electrical signal easy to record either analog or digitally. ^{first such device developed by} The French group consisted of two photoelectric cells measuring the rotation of the light beam reflected by a mirror clamped to a magnet. To reduce power consumption, photo-electric detectors have been replaced by capacitive one.

A third group of variometers comprised devices with saturable cores, using the hysteresis of ferromagnetic materials. If such a material is placed inside a coil and is excited by a sinusoidal magnetic field H , of frequency F , one obtains at the coil terminals, a voltage which contains only odd harmonics. The presence of a field H_0 , added to the field H , creates a signal of frequency $2f$ which cancels out and has its sign changed when H_0 goes across zero. Most of the fluxgates work on this principle, to within some alternatives. The magnetometers are rather compact, reliable and rather sensitive. Their most important drawback is their thermal drift, the variations of temperature changing the electrical properties of the core. Several industrial companies sell equipment measuring the three components of the field with an accuracy of 0.1 to 1 nT and thermal drifts 0.1 to 0.2 nT°C⁻¹. Most of them are equipped with a numerical output, allowing an easy recording of the transient field. On the whole, these devices are well adapted to study the induction phenomena, except at very low frequencies where thermal drifts are particularly disturbing.

A fourth group of devices comprises induction sensors. One more, their principle is very old. The variation of the magnetic field H induce in a coil having a highly permeable ferromagnetic core, an

electromotive force proportional to dH/dt . In order to obtain $H(t)$, the coil must be attached to an integrating device. The main drawback of this system are:

- a decrease of the sensitivity with frequency which makes their use below 10^{-3} Hz very difficult.
- the existence of a resonant frequency of the sensor which creates modulations and phase variations depending on the frequency of the field to be measured.

The use of feedback flux has been an important improvement. One more, the principle lies in the compensation of the natural variations of the field by a current produced by an electronic feed-back system and flowing in an additional coil of some tens of turns. The main coil is used only as a small detector and its characteristics are no longer important. So, with a single coil, it is possible to obtain a flat passband from 3×10^{-4} Hz to several hundreds hertz. Towards higher frequencies one can reach 30 KHz with ferrite cores and 300 KHz with air cores. The noise level is 10^{-1} nT Hz^{1/2} toward 1000 Hz.

Like fluxgates, different kinds of induction variometers are developed industrially for very different purposes. They are reliable devices with a low power consumption, this sensitivity can be quite good provided they are associated to good quality amplifiers. The optimum frequency domain is usually above 1 Hz.

Estimation Z-Matrix from Measured Data

The estimation of the elements of Z-transfer has to be done

in frequency domain while the collected data is in time domain. Thus first the measured variations of E_x , E_y , H_x and H_y have to be transferred to frequency domain. This is usually now done through fast Fourier transform. From this data collected by the system, the one during periods of magnetic activity are selected. One such record from classic paper of Prof. K. Vozoff (Geophysics, vol. 37, 1972) is shown in fig. 1. The power density is of some of the elements are shown in fig. 2. The procedure adopted to estimate the elements of Z are now detailed.

Consider the equation.

$$E_x = Z_{xx} H_x + Z_{xy} H_y$$

Where E_x , H_x , H_y may be considered to be Fourier transforms of measured electric and magnetic field data.

Since any physical measurement of E and H will include some noise, it is usually desirable to make more than two independent measurements, and then to use some type of averaging that will reduce the effects of the noise. Suppose one has n measurements of E_x , H_x , and H_y at a given frequency. One can then estimate Z_{xy} in the sense of least squares. Define

$\Psi = \sum_{i=1}^n (E_{xi} - Z_{xx} H_{xi} - Z_{xy} H_{yi}) (E_{xi}^* - Z_{xx}^* H_{xi}^* - Z_{xy}^* H_{yi}^*)$ where E_{xi}^* is the complex conjugate of E_{xi} , etc. Then find a value of Z_{xx} and Z_{xy} that minimises Ψ . Setting the derivations of Ψ with respect to the real and imaginary parts of Z_{xx} to zero, yields

$$\sum_{i=1}^n E_{xi} H_{xi}^* = Z_{xx} \sum_{i=1}^n H_{xi} H_{xi}^* + Z_{xy} \sum_{i=1}^n H_{yi} H_{xi}^* \quad (III.1)$$

Similarly, setting the derivatives of Ψ with respect to the real and imaginary part of Z_{xy} to zero yields:

$$\sum_{i=1}^n E_{xi} H_{yi}^* = Z_{xx} \sum_{i=1}^n H_{xi} H_{yi}^* + Z_{xy} \sum_{i=1}^n H_{yi} H_{yi}^* \quad (III.2)$$

The summations represent auto and cross power density spectra. Eqs. (III.1) and (III.2) may then be solved simultaneously to get Z_{xx} and Z_{xy} . This solution will minimise the error caused by noise on E_x . It is possible to define other mean squares estimates that minimise other types of noise. For example if one takes,

$$\Psi = \sum_{i=1}^n \left(\frac{E_{xi}}{Z_{xx}} - H_{xi} - \frac{Z_{xy}}{Z_{xx}} H_{yi} \right) \left(\frac{E_{xi}^*}{Z_{xx}^*} - H_{xi}^* - \frac{Z_{xy}^*}{Z_{xx}^*} H_{yi}^* \right)$$

the resulting equation will minimise the error introduced by the noise on H_x .

There are four distinct equations that arise from the various mean square estimates. In terms of the auto and cross power density spectra, they are

$$\overline{E_x E_x^*} = Z_{xx} \overline{H_x H_x^*} + Z_{xy} \overline{H_y H_x^*} \quad (III.3)$$

$$\overline{E_x E_y^*} = Z_{xx} \overline{H_x H_y^*} + Z_{xy} \overline{H_y H_y^*} \quad (III.4)$$

$$\overline{E_x H_x^*} = Z_{xx} \overline{H_x H_x^*} + Z_{xy} \overline{H_y H_x^*} \quad (III.5)$$

$$\text{and } \overline{E_x H_y^*} = Z_{xx} \overline{H_y H_y^*} + Z_{xy} \overline{H_y H_y^*} \quad (III.6)$$

Strictly speaking, Eqs. (III.3) to (III.6) are valid only if $\overline{E_x E_x^*}$, $\overline{E_x E_y^*}$ etc; represent the power density at a discrete frequency, ω . In practice, however, Z_{ij} are slowly varying function of frequency, and as such, $\overline{E_x E_x^*}$ etc. may be taken as average over some finite band width.

They are six possible pairs of equations from (III.3) to (III.6) that can be solved for Z_{xx} and Z_{xy} . Pairs involving (III.3) and (III.6) and the pairs (III.4) and (III.5) are not used since solutions involving these pairs become indeterminate as the lateral inhomogeneity vanishes and the impedance becomes one-dimensional. The apparent resistivity is computed as
$$\rho_{xy} = \frac{0.2}{f} |Z_{xy}|^2 \text{ ohm. meter}$$
 when the units of Z_{xy} are $\frac{mV/Km}{nT}$

Problem of Noise

The various estimates of the elements of Z-matrix are biased either up by random noise on E or down by random noise on H . This is caused by the fact that the auto power density spectra are in general biased up by random noise, while the cross power density spectra are not biased. For examples, suppose that

$$E_x = E_{xs} + E_{xn} \quad (III.7)$$

$$H_y = H_{ys} + H_{yn} \quad (III.8)$$

$$\text{where } \langle E_{xs} E_{xn}^* \rangle = 0 \quad (III.9)$$

$$\langle H_{ys} H_{yn}^* \rangle = 0 \quad (III.10)$$

$$\langle E_{xn} H_{yn}^* \rangle = 0 \quad (III.11)$$

and where brackets denote "expected value of". Clearly, for this situation

$$\langle E_x E_x^* \rangle = \langle E_{xs} E_{xs}^* \rangle + \langle E_{xn} E_{xn}^* \rangle \quad (III.12)$$

$$\langle H_y H_y^* \rangle = \langle H_{ys} H_{ys}^* \rangle + \langle H_{yn} H_{yn}^* \rangle \quad (III.13)$$

$$\text{and } \langle E_x H_y^* \rangle = \langle E_{xs} H_{ys}^* \rangle \quad (III.14)$$

Eqn. (III.14) suggests that the cross power can be estimated to any arbitrary degree of accuracy by measuring the fields for a long enough period of time. On the other hand (III.12) and (III.13) imply that the estimates of the auto powers will be

biased regardless of the length of time for which the fields are measured. Now, suppose, that one performs two simultaneous independent measurements of one of the field component, say E_x if the results are:

$$E_{x1} = E_{xs} + E_{xn1} \quad (III.15)$$

$$\text{and } E_{x2} = E_{xs} + E_{xn2} \quad (III.16)$$

$$\text{where } \langle E_{xs} E_{xn1}^* \rangle = 0 \quad (III.17)$$

$$\langle E_{xs} E_{xn2}^* \rangle = 0 \quad (III.18)$$

$$\text{and } \langle E_{xn1} E_{xn2}^* \rangle = 0$$

$$\text{then } \langle E_{x1} E_{x2}^* \rangle = \langle E_{xs} E_{xs}^* \rangle \quad (III.19)$$

Eqn. (III.19) implies that the E_x auto power density spectrum can be estimated to any arbitrary degree of accuracy from two simultaneous noisy measurements of E_x if measurements are taken for a long enough period of time and if the noise on the two measurements are independent.

In general, if one has double measurements of either the two tangential components of E or the two tangential components of H , one can obtain estimate of the four elements of the Z - matrix that are not biased by random noise.

Computation of Depth Conductivity Profile

The geophysical interest lies in determining material properties of the earth's interior from data obtained on the earth's surface. The approach here is to parameterize the earth as a series of horizontal layers of constant resistivity. The problem is then one-dimensional. Alternative approaches based on a parameterization where the earth has a continuous resistivity profile have been formulated by Bostick (1977) and Oldenberg (1979: Geophysics vol. 44). Two - dimensional inverse

problem has only recently been possible.

We discuss here the one - dimensional case. Most of the work concern with earth in terms of finite-layered model. Since the resulting inversion problem is non-linear, workers proceed to locally linearize the problems and use a Newton type method of iteration. The advantage of a finite dimensional space of unknowns lies in the computational simplicity introduced in that process may be described in the simpler terms of matrices.

In formulating the magneto-telluric inverse problem, we start with the observations $P_a^*(\omega)$, $\theta_a^*(\omega)$. These are determined from estimate of the tensor elements.

$$P_a = \frac{|Z_1|}{\omega \mu} \quad \theta_a = \tan^{-1} [Im(Z_1)/Re(Z_1)]$$

For 2 - or 3 - dimensional cases, we take estimates of tensor elements for those principal directions which seems to lead to valid one-dimensional models. The determination of the data may be very difficult problem in some cases and may not have an obvious resolution in others. For a strictly two-dimensional situation, workers generally, chose the parallel resistivity and phase estimates as the most representative on which to invert. For data contaminated by surficial three-dimensional effects, we may have to adjust the entire response curve in some way as to strip away these surficial features.

We start with our observations, which are a function of frequency, and derive a one-dimensional model giving resistivity as a function of depth consider the observations:

$$Y^* = \begin{bmatrix} P_{a,1}^* \\ P_{a,2}^* \\ \vdots \\ P_{a,k}^* \\ \theta_{a,1}^* \\ \theta_{a,2}^* \\ \vdots \\ \theta_{a,k}^* \end{bmatrix} = \begin{bmatrix} y_1^* \\ y_2^* \\ \vdots \\ y_k^* \\ y_{k+1}^* \\ y_{k+2}^* \\ \vdots \\ y_m^* \end{bmatrix} \quad m = 2k \quad (III.20)$$

We have in addition, specified model consisting of layer resistivities and thickness and may represent these parameters by a vector X consist of

$$X = \begin{bmatrix} \rho_1 \\ \rho_2 \\ \vdots \\ \rho_l \\ d_1 \\ d_2 \\ \vdots \\ d_{l-1} \end{bmatrix} = \begin{bmatrix} x_1^* \\ x_2^* \\ \vdots \\ x_l^* \\ x_{l+1}^* \\ \vdots \\ x_n^* \end{bmatrix} \quad n = 2l-1 \quad (III.21)$$

Using equation given in lecture-1, we define a functional relationship between the model parameters, x_j and the response parameters, y_i which has the form

$$y_i = F_i(x_j) \quad (III.22)$$

for the magnetotelluric problem this functional is highly non-linear and we proceed to linearize the problem by expanding equation (III.22) about the model X in a Taylor's series, giving:

$$(y_i^* - y_i) = \sum_{j=1}^n \frac{\partial y_i}{\partial x_j} \Delta x_j \quad (III.23)$$

Equation (III.23) can be written in matrix notation as:

$$A \Delta X = \Delta Y \quad (III.24)$$

where the matrix A is referred to as the Jacobian, partial derivative, on sensitivity matrix, and has elements defined by

$$A_{ij} = \frac{\partial y_i}{\partial x_j} \quad (III.25)$$

In magnetotellurics a transformation of model parameters to a logarithmic representation is often made. In the case discussed here only the apparent resistivity data is transformed to a logarithmic representation. The advantage of such a step is:

- it facilitates interpretation done from master curves, which are usually in logarithmic variables,
- it makes the observational errors in apparent resistivity approximately constant,
- the representation reflects a sensitivity decreasing exponentially with depth,
- the problem is linearized to a certain extent with a resulting decrease in the number of iterations needed to obtain a satisfactory solution,
- the natural condition of having all parameters constrained to be greater than Zero is automatically met,
- the partial derivative matrix A is non-dimensionalized except for the phase derivatives.

The changes to equations (III.20) and (III.21) of our matrix formulation are there

$$Y^o = \left(\frac{\log P_a}{\sigma_a} \right) \quad (III.26)$$

$$X^o = \left(\frac{\log P}{\log d} \right) \quad (III.27)$$

and the associated partial derivative matrix A is now defined as:

$$A_{ij} = \begin{pmatrix} \frac{\partial \log P_{a,i}}{\partial \log P_j} & \frac{\partial \log P_{a,i}}{\partial \log d} \\ \frac{\partial \log P_{a,v}}{\partial \log P_j} & \frac{\partial \log P_{a,v}}{\partial \log d} \end{pmatrix} \quad (III.28)$$

To illustrate the application of the technique, the example from magneto-telluric measurements made in the Hueco Botson near El Paso, Texas in the southern Rio Grande rift Zone is discussed (Pederson and Hermance, Survey in Geophysics, 8, 1986, 187-231). Although there are problems with high skewness coefficients for this data (0.3 - 0.7), nevertheless the strike direction is in line with the geological strike of the sedimentary basins in this region. Assuming that the high skewness is caused by surficial features in such a way as not to affect the longer period data, we may represent the region as a two-dimensional structure and invert on the apparent resistivity measured parallel to strike. In fig. 3 and 4, the parallel apparent resistivity and phase data along with the associated error bars are displayed. A five layered model was found to fit the apparent resistivity data in a best least-square sense and the model is shown in fig. 5. The technique used was generalized inversion as summarized below.

We now take up as to how exactly the optimal model is found from the observed data, Rewrite equation (III.24)

$$A \Delta X = \Delta Y \quad (III.29)$$

This relation will be useful to find a solution X_1^{new} that provides best fit to the data where

$$X_1^{\text{new}} = X_1^{\text{old}} + \Delta X \quad (III.29)$$

We start with some initial model parameters X_0 ; solve equation (III.24)

for ΔX and use equation (III.29) to find a new model. This new model is recycled back into equation (III.24) and the process is repeated with various convergence criteria are met. The interaction process is needed because of the non-linearity of the functional dependence as shown in equation (III.22). We define a best fit in terms of a least squares minimization of

$$Q = \| A \Delta X - \Delta Y \|^2 \quad (\text{III.30})$$

Dimension of matrix A is $m \times n$, where m is number of observations and n is the number of unknown model parameters. Rank of A is less than or equal to min of m and n . If the matrix A has full column rank, $r(A)=n$, then the least squares solution of equation (III.24) is given by the normal equation.

$$\Delta X = (A^T A)^{-1} A^T \Delta Y \quad (\text{III.31})$$

If the rank is less than n , a solution may be found by selecting among all least squares solution, one which is closest to the reality.

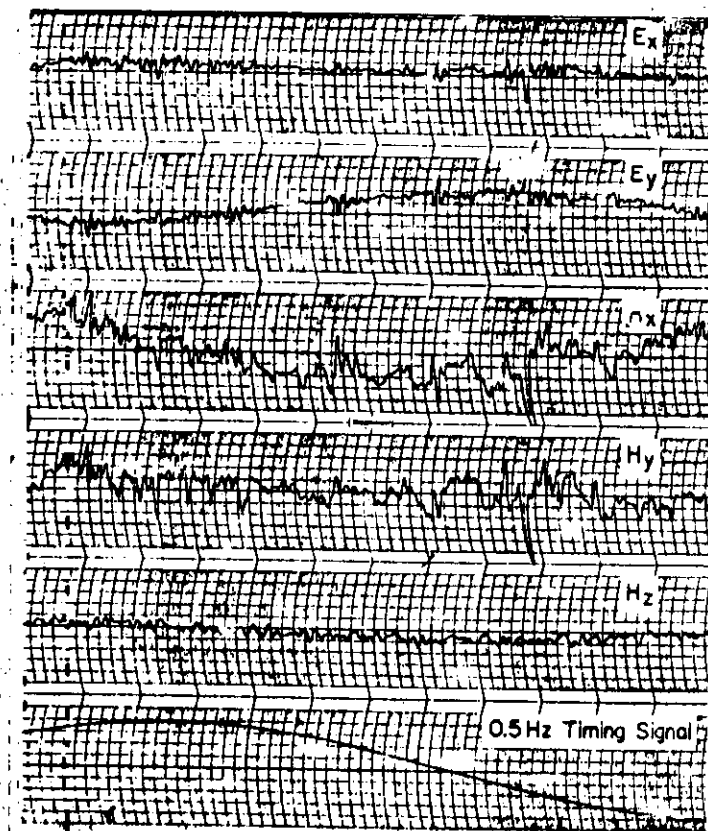
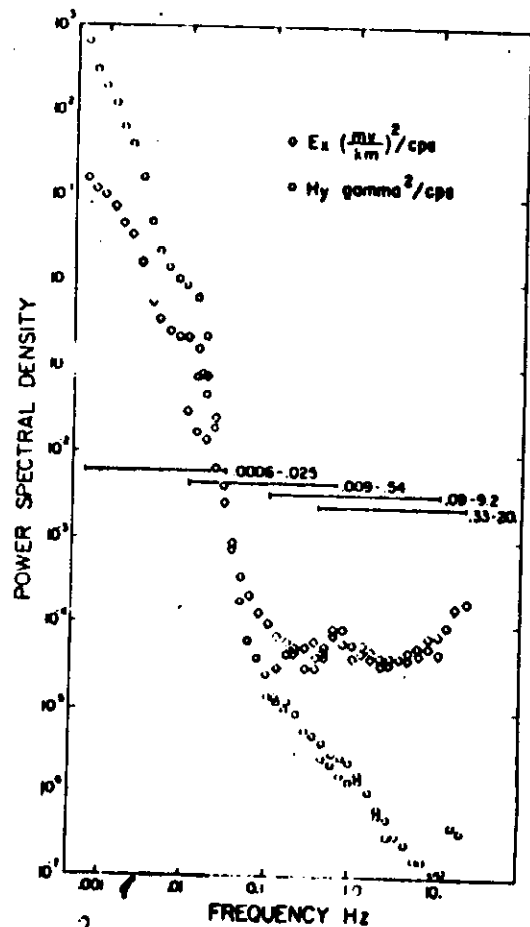
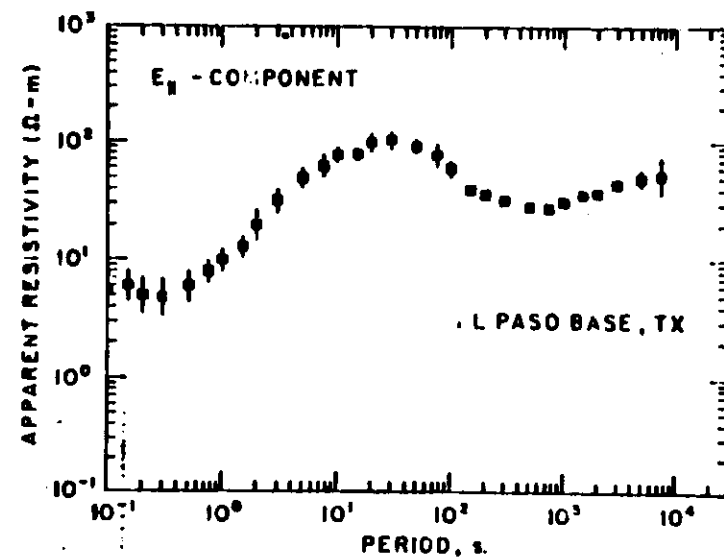


Fig. 1. Typical noise-like telluric signals. Sine wave at bottom shows time scale.



2
Fig. 2. Selected power spectral densities recorded in the four overlapping frequency bands indicated. Bands were recorded at different times.



3
Fig. 3. Apparent resistivity versus period for a magnetotelluric site in the southern Rio Grande rift zone near El Paso, Texas. The data shown is the maximum principal resistivity which was determined to be the parallel component.

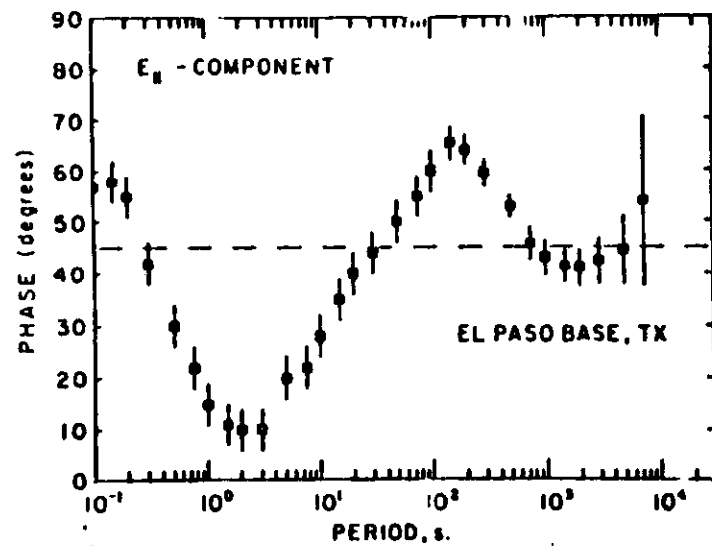


Fig. 4. Phase versus period for same magnetotelluric site as in Figure 2. The data are associated with the parallel (maximum) resistivity component in the principal coordinates.

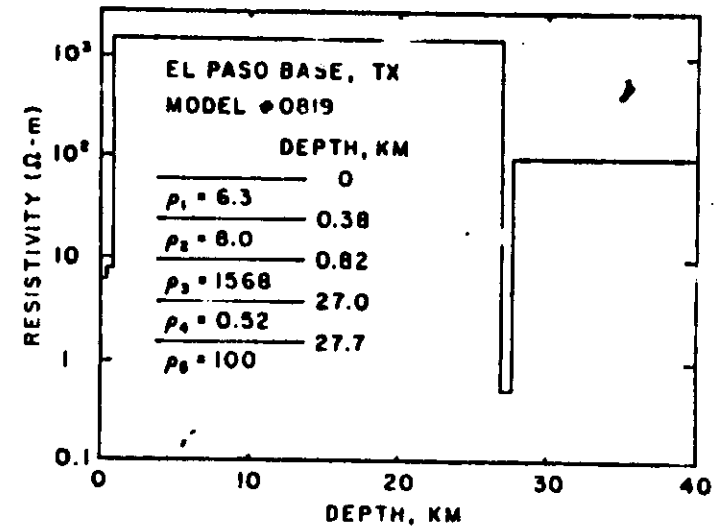


Fig. 5. Optimum five layer model fitting the apparent resistivity data of Figure 2 as determined by a nonlinear least squares inversion routine.